

On-Line Supporting Information

Random Walk of Single Gold Nanoparticles in Zebrafish Embryos Leading to Stochastic Toxic Effects on Embryonic Developments

Lauren M. Browning[†], Kerry J. Lee[†], Tao Huang, Prakash D. Nallathamby, Jill E. Lowman,
and Xiao-Hong Nancy Xu^{*}

Department of Chemistry and Biochemistry, Old Dominion University, Norfolk, Virginia 23529

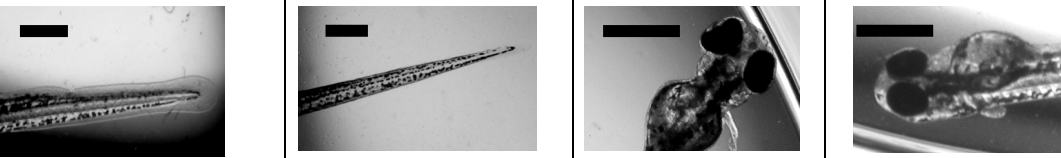
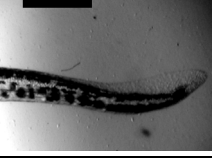
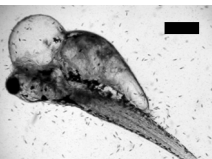
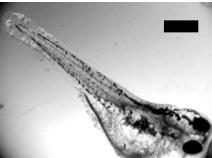
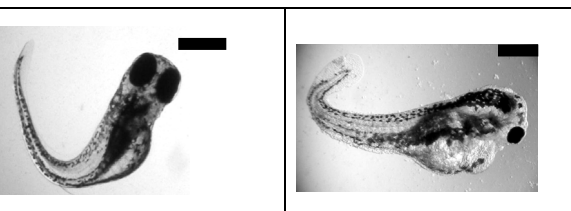
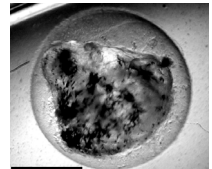
The on-line SI includes:

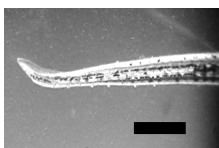
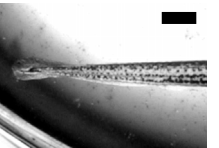
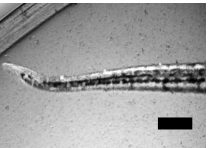
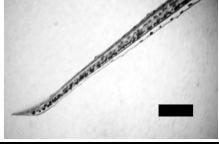
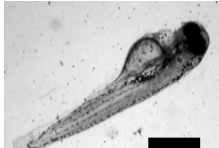
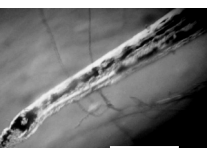
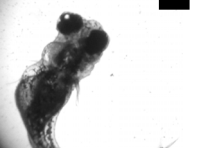
- (1) One table (**Table 1S**) summarizes representative deformities of zebrafish that were treated chronically at cleavage stage for 120 h with given concentrations of Au nanoparticles, illustrating that deformities of zebrafish show random dependence on Au nanoparticle concentration.
- (2) One figure (Figure 1S) shows the characterization and analysis of concentrations of unwashed, the first-time washed and the second-time washed Au nanoparticle solutions.
- (3) One figure (Enlarged Figure 5A:b-e in the text) illustrates single Au nanoparticles with multiple colors embedded in the tissues of (b) the top and (c) bottom of the chorionic surface, (d) in chorionic space and (e) in inner mass of the embryo.

[†] These authors contributed equally to this work.

* To whom correspondence should be addressed: Email: xhxu@odu.edu; www.odu.edu/sci/xu/xu.htm; Tel/fax: (757) 683-5698

Table 1S: Representative deformities of zebrafish that were treated chronically at cleavage stage for 120 h with given concentrations of Au nanoparticles, illustrating that deformities of zebrafish depend randomly on Au nanoparticle concentration.

C (nM)	Images
0	<p style="text-align: center;">Control (Normal Development)</p> 
0.025	<p style="text-align: center;">Finfold Abnormality* and Tail/Spinal Cord Flexure*</p> 
0.10	<p style="text-align: center;">Cardiac Malformation* and Yolk Sac Edema*</p> 
0.20	<p style="text-align: center;">Finfold Abnormality</p>  <p style="text-align: center;">Finfold Abnormality*, Tail/Spinal Cord Flexure*, Cardiac Malformation*, Yolk Sac Edema*</p>  <p style="text-align: center;">Cardiac Malformation*, Yolk Sac Edema*, No Tail* and Acephaly*</p> 

	Finfold Abnormality* and Tail/Spinal Cord Flexure*
0.40	
0.80	Finfold Abnormality
	
	Finfold Abnormality* and Tail/Spinal Cord Flexure*
	
	Finfold Abnormality* and Tail/Spinal Cord Flexure*
1.00	
	Finfold Abnormality*, Tail/Spinal Cord Flexure*, Cardiac Malformation*, Yolk Sac Edema*
	
	Finfold Abnormality* and Tail/Spinal Cord Flexure*
1.20	
	Finfold Abnormality*, Tail/Spinal Cord Flexure*, Cardiac Malformation*, Yolk Sac Edema*
	

* Multiple types of deformities are observed in a single zebrafish.

The scale bar = 500 µm

Figure 1S

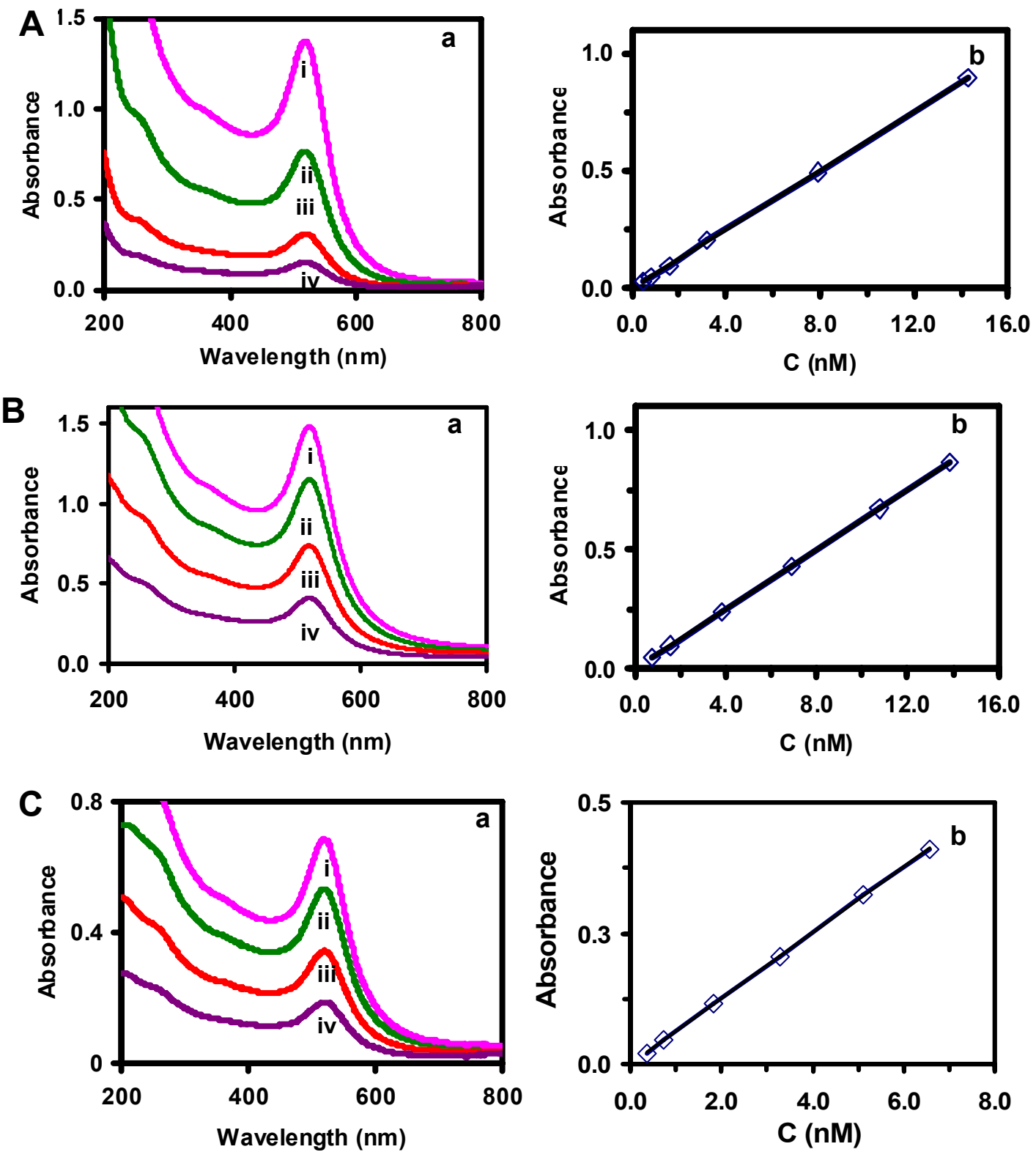


Figure 1S. Determination of concentrations of (A) unwashed, (B) the first-time washed, and (C) the second-time washed Au nanoparticle solutions:

- (A) (a) UV-Vis absorption spectra of (11.6 ± 0.9) nm unwashed Au nanoparticles show background-subtracted absorbance at (i) 0.894, (ii) 0.496, (iii) 0.202, and (iv) 0.097 with peak wavelength (λ_{\max}) of 520 nm.
- (b) Plot of absorbance versus concentration of nanoparticles in (a) shows a linear calibration curve with a linear regression of 1.0 and extinction coefficient ($\epsilon_{520 \text{ nm}}$, molar absorptivity) of $6.3 \times 10^7 \text{ M}^{-1} \text{ cm}^{-1}$.
- (B) (a) UV-Vis absorption spectra of the first-washed Au nanoparticles show background-subtracted absorbance at (i) 0.868, (ii) 0.672, (iii) 0.431, and (iv) 0.240, with a peak wavelength (λ_{\max}) of 520 nm.
- (b) Plot of absorbance versus concentration of nanoparticles in (a) shows a linear calibration curve with a linear regression of 1.0 and extinction coefficient ($\epsilon_{520 \text{ nm}}$, molar absorptivity) of $6.3 \times 10^7 \text{ M}^{-1} \text{ cm}^{-1}$.
- (C) (a) UV-Vis absorption spectra of the first-washed Au nanoparticles show background-subtracted absorbance at (i) 0.411, (ii) 0.323, (iii) 0.205, and (iv) 0.115 with a peak wavelength (λ_{\max}) of 520 nm.
- (b) Plot of absorbance versus concentration of nanoparticles in (a) shows a linear calibration curve with a linear regression of 1.0 and extinction coefficient ($\epsilon_{520 \text{ nm}}$, molar absorptivity) of $6.3 \times 10^7 \text{ M}^{-1} \text{ cm}^{-1}$.

Figure 5A

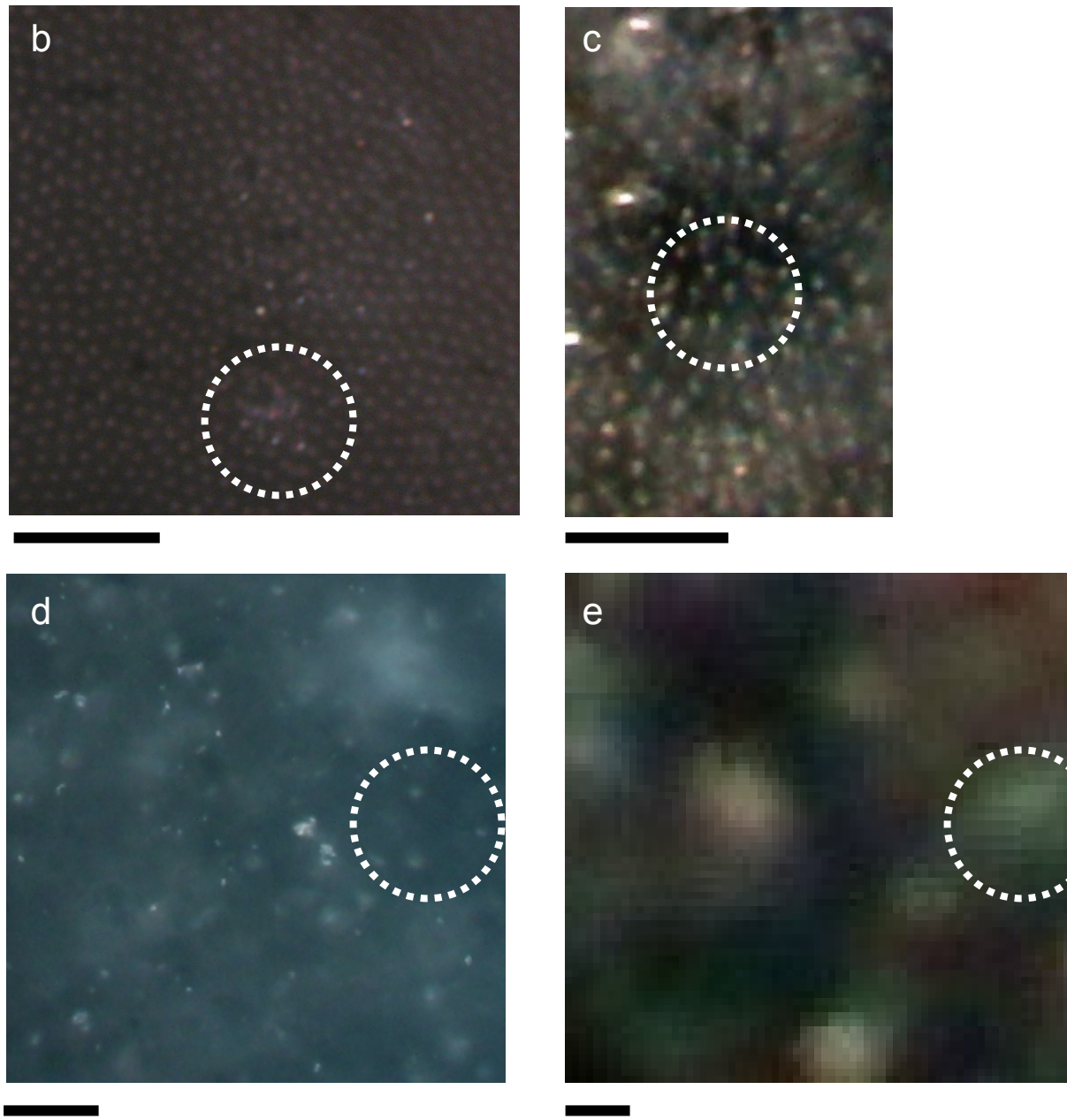


Figure 5A (b-e): Enlarged figures of Figure 5A (b-c) in the text, showing single Au nanoparticles with multiple colors in (b) the top and (c) bottom of the chorionic surface, showing well-organized chorionic pores; (d) in chorionic space and (e) in inner mass of the embryo. The dark-background is the tissue, and the colors are contributed by localized surface plasmon resonance (LSPR) spectra of Au nanoparticles, similar to those observed in Figure 2C. Note that the unique feature of LSPR spectra of single Au nanoparticles allows us to distinguish them from any possible tissue debris or vesicle-like particles in embryos.